JOURNAL OF VIROLOGY, Nov. 2002, p. 11505–11517 Vol. 76, No. 22
0022-538X/02/$04.00+0 DOI: 10.1128/JVI.76.22.11505–11517.2002


# Adenovirus-Facilitated Nuclear Translocation of Adeno-Associated Virus Type 2

Wu Xiao,[1,2] Kenneth H. Warrington, Jr.,[1,3] Patrick Hearing,[4] Jeffrey Hughes,[1,2] and Nicholas Muzyczka[1,3]*

*Powell Gene Therapy Center[1] and Department of Molecular Genetics and Microbiology,[3] University of Florida College of Medicine, and Department of Pharmaceutics, University of Florida College of Pharmacy,[2] Gainesville, Florida 32610, and Department of Molecular Genetics and Microbiology, SUNY Stony Brook University, Stony Brook, New York 11794[4]*

Received 3 May 2002/Accepted 31 July 2002

**We examined cytoplasmic trafficking and nuclear translocation of adeno-associated virus type 2 (AAV) by using Alexa Fluor 488-conjugated wild-type AAV, A20 monoclonal antibody immunocytochemistry, and subcellular fractionation techniques followed by DNA hybridization. Our results indicated that in the absence of adenovirus (Ad), AAV enters the cell rapidly and escapes from early endosomes with a $t_{1/2}$ of about 10 min postinfection. Cytoplasmically distributed AAV accumulated around the nucleus and persisted perinuclearly for 16 to 24 h. Viral uncoating occurred before or during nuclear entry beginning about 12 h postinfection, when viral protein and DNA were readily detected in the nucleus. Few, if any, intact AAV capsids were found in the nucleus. In the presence of Ad, however, cytoplasmic AAV quickly translocated into the nucleus as intact particles as early as 40 min after coinfection, and this facilitated nuclear translocation of AAV was not blocked by the nuclear pore complex inhibitor thapsigargan. The rapid nuclear translocation of intact AAV capsids in the presence of Ad suggested that one or more Ad capsid proteins might be altering trafficking. Indeed, coinfection with empty Ad capsids also resulted in the appearance of AAV DNA in nuclei within 40 min. Escape from early endosomes did not seem to be affected by Ad coinfection.**

Adeno-associated virus type 2 (AAV) is the prototypical helper-dependent parvovirus (26). Like the related autonomous parvoviruses, AAV capsids are icosohedral (approximately 20 nm in diameter) and package a 4.7-kb single-stranded DNA genome. DNA replication and viral packaging occur in the nuclei of infected cells, and thus the first step in the viral life cycle is the delivery of viral DNA to the host nucleus.

Several groups have examined the steps involved in this process (4, 6–8, 15–17, 30, 34, 35, 40, 41). Heparin sulfate proteoglycan, the first receptor identified for AAV (41), appears to function primarily in virus attachment to the cell surface. Efficient AAV infection also appears to require a second coreceptor, such as human fibroblast growth factor receptor type 1 (30) or integrin $\alpha_v\beta_5$ receptor (34, 40). AAV then enters cells through receptor-mediated endocytosis in clathrin-coated pits, and this event requires dynamin, a 100-kDa cytosolic GTPase that selectively regulates clathrin-mediated endocytosis (4, 7).

In general, AAV trafficking appears to be similar within the first 2 h to that of the autonomous parvoviruses (references 44 and 49 and references therein). There appears to be a need for early endosome acidification since inhibitors of the vacuolar $H^+$-ATPase such as bafilomycin $A_1$ or treatment of cells with $NH_4Cl$ reduces trafficking to the nucleus and inhibits AAV transduction (4, 6, 16, 27). Interaction of AAV with the $\alpha_v\beta_5$ receptor apparently leads to activation of Rac1 and phosphatidylinositol 3-kinase both of which are necessary for efficient trafficking to the nucleus. Inhibition of Rac1 by a dominant negative mutant or inhibition of phosphatidylinositol 3-kinase with wortmannin leads to a significant reduction in the trafficking of virus to the nucleus (34). Microtubule and microfilament disruptors (nocodazole and cytochalasin B) also reduce the nuclear accumulation of virus (34).

Inhibitor studies with brefeldin A, a fungal antibiotic that causes early endosomes to form a tubular network, suggested that virus might transition to late endosomes (6). This observation was confirmed by density gradient fractionation of cytoplasmic vesicles (16). Virus appeared to accumulate within the first 2 h postinfection in dense, acidic, β-galactosidase-containing endosomes, the so-called late endosomes. However, other studies suggested that the virus was released from early endosomes into the cytoplasm. Bartlett et al. (4) demonstrated that lysosomotropic agents such as ammonium chloride inhibited AAV transduction only during the first 30 min after infection. Seisenberger et al. (35) used-real time single-molecule imaging of labeled virus to demonstrate that a substantial fraction of virus had a diffusion coefficient consistent with free virus in the cytoplasm shortly after infection. Thus, the question whether the virus goes through a late endosome has not yet been resolved. Additionally, two groups (6, 8) have demonstrated that proteosome inhibitors led to an increase in both intracellular accumulation of DNA and recombinant AAV (rAAV)-mediated transduction. This suggested that ubiqitination of rAAV interferes with rAAV transduction, something that usually occurs outside an endosomal compartment. However, proteosome inhibition does not uniformly increase trans-

* Corresponding author. Mailing address: Department of Molecular Genetics and Microbiology, College of Medicine, University of Florida, P.O. Box 100266 JHMHSC, Gainesville, FL 32610. Phone: (352) 392-8541. Fax: (352) 392-5914. E-mail: muzyczka@ufl.edu.

duction in all cell types (8), and it is now clear that there may be alternative trafficking methods. Hansen et al. (15, 16) have shown that NIH 3T3 cells, which normally are not easily transduced with rAAV, accumulate virus at an early endosome step, in contrast to 293 cells. Treatment with hydroxyurea increased virus accumulation in late endosomes by an unknown mechanism. Additionally, Nicklin et al. (27) have recently shown that if the tropism of the virus is changed to recognize a different cell surface receptor, it is no longer sensitive to bafilomycin inhibition during infection.

Surprisingly, unlike adenovirus (Ad), the next step in trafficking, entry into the nucleus, appears to be particularly slow. Some investigators have commented on the fact that the bulk of the virus persists in a perinuclear location up to 4 h postinfection (4, 11). However, other investigators have argued that viral DNA can be found in the nucleus within 2 h as either DNA or intact virus particles (15, 34), or as soon as 15 min after infection (35). The question whether intact AAV particles enter the nucleus is also not yet resolved. It remains unclear whether virus uncoats in the nucleus, in the cytoplasm, or in the endosome. Hansen et al. (17) demonstrated that viral DNA and labeled viral protein could penetrate cell free nuclei by a mechanism that did not appear to require nuclear pore complexes (NPC). Finally, limited studies have been done in the presence of the helper virus, Ad. Coinfecting cells with Ad does not result in any influence on the AAV infectious pathway within the first 2 to 4 h after infection (4). Fluorescently labeled AAV accumulates perinuclearly within 2 h regardless of whether Ad is included in the infection.

In this study, we reexamined trafficking in HeLa cells of highly purified wild-type AAV in the presence and absence of Ad by using fluorescently labeled virus, monoclonal antibodies that recognize only intact AAV particles, and DNA hybridization. We found a dramatic difference in AAV trafficking depending on whether Ad is present during the infection. In the absence of Ad, AAV persists perinuclearly for up to 24 h and little if any intact virus enters the nucleus. In contrast, when Ad is present, intact AAV particles enter the nucleus within 40 min. Additionally, entry into the nucleus in the presence of Ad occurs even in the presence of a nuclear pore inhibitor, and, regardless of whether Ad is present, virus appears to escape from early endosomes shortly after infection.

## MATERIALS AND METHODS

**Cell culture.** HeLa cells and HEK 293 cells were obtained from the American Type Culture Collection (Manassas, Va.) and grown at 37°C in a 5% $CO_2$ atmosphere in Dulbecco's modified Eagle's medium (DMEM) supplemented with 10% fetal calf serum, 100 U of penicillin per ml, and 100 U of streptomycin per ml. For NPC inhibition studies, the medium was replaced by $Ca^{2+}$-free S-MEM (Gibco-BRL, Grand Island, N.Y.).

**Production of virus.** Ad5 was produced as described previously (48). Empty Ad capsids were produced with Ad5 *ts*369 (18) grown in 293 cells at the restrictive temperature of 39.5°C. The empty capsids were banded three times on CsCl gradients, and the particle concentration was determined by measurement of absorbance at 280 nm and comparison to known protein standards. Wild-type AAV was generated from plasmid pSM620 as described previously (32). AAV was purified by iodixanol step gradient and heparan sulfate affinity chromatography as described (48, 50). Viral stocks were subjected to titer determination by a DNA slot-blot method (29), except that the hybridization probe was synthesized from the *Xba*I fragment of plasmid pIM45 (25), using the North2South biotin random prime kit (Pierce, Rockford, Ill.) and the membrane was developed using the North2South chemiluminescent nucleic acid hybridization and detection kit (Pierce). The purity of the labeled virus was assessed by electron microscopy (29) and sodium dodecyl sulfate-polyacrylamide gel electrophoresis (SDS-PAGE) followed by Coomassie blue staining or immunoblotting (48) (see Fig. 1).

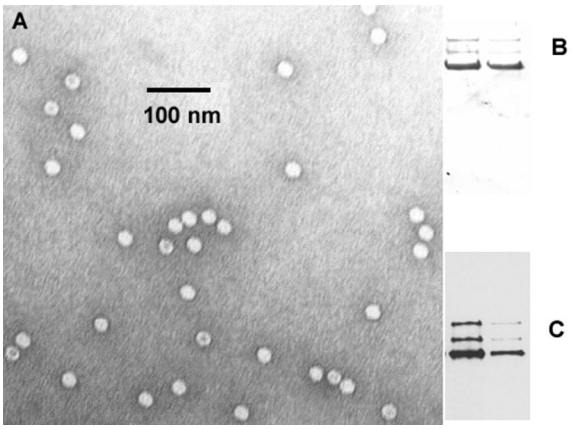


FIG. 1. Characterization of AAV preparations. (A) Electron micrograph of wild-type AAV used in this study. Particles with a black dot in the center are likely to be empty capsids. (B and C). Coomassie blue staining (B) and Western blotting (C) of wild-type AAV capsid preparations that had been fractionated on SDS-acrylamide gels. In each gel, the left lane contained $10^{11}$ particles and the right lane contained $10^{10}$ particles. The Western blot was detected with anti-capsid B1 monoclonal antibody (31, 47).

**Fluorescent labeling of AAV and viral infection of HeLa cells.** AAV stocks were labeled with Alexa Fluor 488 fluorescent dye using a protein-labeling kit (Molecular Probes, Eugene, Oreg.). Labeled virus was dialyzed extensively against 10 mM Tris (pH 7.8)-150 mM NaCl with 10% glycerol (4) and further purified by heparin column chromatography as described above. The dye-to-viral-particle ratios of the Alexa Fluor 488-labeled AAV preparations were calculated as previously described (3) using the manufacturer's extinction coefficient for Alexa Fluor 488; they were found to be 2.

HeLa cells were grown to 70% confluence in 35-mm culture dishes containing 22-mm coverslips (Fisher Scientific, Atlanta, Ga.), which had been pretreated with 50 μg of type 1 rat tail collagen (Collaborative Biomedical Products, Bedford, Mass.) per ml in 0.02 M acetic acid. The cells were infected with the purified fluorescent AAV at a multiplicity of infection (MOI) (1) of 10,000 DNA-containing particles per cell by a modification of a method described previously (3, 4, 22). Cells were exposed to the virus for 10 min at 37°C in serum-free binding buffer (DMEM supplemented with 10 mM HEPES [pH 7.3] and 1% bovine serum albumin), washed twice with binding buffer and once with serum-containing DMEM (DMEM containing 10% fetal calf serum, 100 U of penicillin per ml, and 100 U of streptomycin per ml), and incubated further at 37°C in the serum-containing DMEM for the indicated time. For Ad coinfection, cells were exposed to Ad5 at a MOI of 10 PFU per cell (approximately 200 DNA-containing particles per cell). Cell samples taken at each time point were washed three times with binding buffer and twice with phosphate-buffered saline (PBS) before being fixed with 4% paraformaldehyde for 10 min at room temperature. Fixed cells were then stained with 1 μM Syto 64 red fluorescent dye (Molecular Probes) for 30 min at room temperature as specified by the manufacturer, and mounted on glass slides using VectaShield fluorescent mounting medium (Vector Laboratories, Inc., Burlingame, Calif.). For control experiments, cells were treated with free dye solution in the same way as they were treated with fluorescent AAV, using 0.1 μl of the free dye stock solution, which gave approximately the same amount of fluorescent signal as the labeled virus did. To localize the nuclei, fixed cells were stained with 1 μg of DAPI (4′,6-diamidino-2-phenylindole [Molecular Probes]) per ml for 5 min at room temperature and visualized by a Zeiss Axioplan 2 fluorescence microscope (4).

**Immunocytochemistry.** Immunocytochemistry was performed using unlabeled AAV based on a published method (34) with A20 monoclonal antibody as the primary antibody and Cy3-labeled goat anti-mouse immunoglobulin G (IgG) (Amersham Pharmacia Biotech, Piscataway, N.J.) as the secondary antibody. Cells were infected with unlabeled virus as described above for fluorescently labeled virus, using the same MOI, the same 10-min incubation time at 37°C, and the same washing procedure. Cells were fixed at the indicated times with 100%

methanol for 10 min at − 20°C before being stained with antibody. In some treatments, cell nuclei were stained with 100 nM Syto X green nucleic acid stain (Molecular Probes) as specified by the manufacturer. Disrupted capsid proteins fractionated on SDS-acrylamide gels were visualized by staining with B1 monoclonal antibody (see Fig. 1). A20 and B1 antibodies (31, 47) were kindly supplied by Jurgen Kleinschmidt (German Cancer Center, Heidelberg, Germany).

**Confocal microscopy.** Confocal microscopy was performed on a 1024 ES confocal microscope (Bio-Rad, Hercules, Calif.). For each sample, a series of 0.5-μm horizontal sections were made through the cells and images representative of the central five or six layers were collected and combined into one picture. The images at all time points were collected under identical conditions and at identical settings. The Syto 64 red fluorescent color was then reduced uniformly prior to printing the confocal photographs to better visualize the green viral signal.

**Detection of viral DNA from cytoplasmic and nuclear fractions of HeLa cells.** HeLa cells were seeded in 35-cm dishes and infected by AAV with or without Ad coinfection as described above. After two washes with binding buffer and one wash with PBS, the cells were trypsinized at 37°C for 10 min, washed twice with 1 ml of PBS, and fractionated into cytoplasmic and nuclear fractions as described previously (24, 39). The purity of each fraction was tested by immunoblotting for the presence the nuclear antigen histone H3 by using an anti-histone H3 polyclonal antibody (Upstate Biotechnology, Lake Placid, N.Y.) and by assaying for the presence of the cytoplasmic enzyme acid phosphatase (EnzChek acid phosphatase assay kit; Molecular Probes) as described previously (15). Viral DNA in each sample was treated with protease, isolated by the Hirt method (19), and visualized by slot blotting as described above. Ad coinfection was performed as described above, except that when empty Ad capsids were used, the MOI was 1,000 particles per cell. When the NPC inhibitor thapsigargin (Sigma, St. Louis, Mo.) was used, cells were pretreated with 0.5 μg of thapsigargin per ml in culture medium at 37°C for 30 min (12, 20), and this concentration of thapsigargin was maintained in the medium during all the following incubations. Films were scanned using a Gel Doc 2000 gel documentation system (Bio-Rad), and signal densities were measured by Quantity One quantitation software version 4.2 (Bio-Rad). The fraction of total DNA in the nucleus was then calculated.

**Subcellular fractionation.** HeLa cells were seeded in 10-cm dishes and allowed to grow to 90% confluence. Virus was added to cells at an MOI of $10^5$ DNA-containing particles per cell in serum-free binding buffer, and the cells were incubated at 37°C for 10 min, with or without Ad at an MOI of 10 PFU per cell. After the initial 10-min exposure, the cells were washed twice with binding buffer and once with serum containing DMEM and incubated in serum-containing DMEM with or without Ad (MOI = 10) at 37°C for the indicated periods. In some experiments, cells were incubated for 1 h at 4°C immediately after addition of virus or were precooled to 4°C for 10 min before addition of virus and then incubated at 4°C for 1 h. Homogenization of cells was performed as described previously (17). Briefly, cell samples were washed twice with binding buffer and twice with PBS and trypsinized at 37°C for 10 min. The cells were washed twice with 10 ml of ice-cold PBS and once with 10 ml of ice-cold homogenization buffer (0.25 M sucrose, 10 mM triethanolamine [23], 1 mM EDTA, 1 mM phenylmethylsulfonyl fluoride, 10 μg of aprotinin per ml) and homogenized in a Kontes Dounce tissue grinder (Fisher Scientific) at 4°C until about 80% cell lysis was achieved as monitored by trypan blue uptake. The nuclear-free cytoplasmic fraction (postnuclear supernatant [PNS]) was collected as described previously (17) and diluted to 6 ml with homogenization buffer. Each 6-ml PNS sample was mixed with an equal volume of 60% iodixanol (Gibco-BRL) and centrifuged at 200,000 × *g* in an SW41 Ti ultracentrifuge rotor at 15°C for 24 h to form a 30% continuous iodixanol gradient (29). Twelve fractions (1 ml each) were collected from the bottom of each tube, and the density of each fraction was determined by weight. Viral DNA was isolated from each fraction as described previously (15, 21). Briefly, each fraction was mixed with equal volume of 1 M NaOH and heated at 65°C for 1 h to release viral DNA. Samples were then extracted once with phenol-chloroform-isoamyl alcohol (Invitrogen, Carlsbad, Calif.) and once with chloroform, mixed with an equal volume of 20× SSC solution (IX SSC is 0.15 M NaCl plus 0.015 M sodium citrate), and analyzed as described above using a dot blot apparatus (Bio-Rad). For ultracentrifugation of free virus, about $10^7$ viral particles were diluted in 6 ml of homogenization buffer, mixed with 6 ml of 60% iodixanol, and centrifuged as above. Viral DNA from each fraction was then isolated and detected as described above. Films were scanned using a Gel Doc 2000 gel documentation system (Bio-Rad), and signal densities were measured by using Quantity One quantitation software version 4.2 (Bio-Rad).

**Analysis of markers for endocytic organelles.** Markers were analyzed for endocytic organelles by minor modifications of a previously described method (16). Briefly, early endosomes were labeled by pulsing the cells with 50 μg of biotinylated human holotransferrin (Molecular Probes) per ml at 37°C in serum-containing DMEM for 10 min. The cells were then homogenized and centrifuged as described above. A 30-μl sample of each fraction was boiled in SDS sample buffer and loaded onto a NitroBind nitrocellulose membrane (Fisher Scientific) through a dot blot apparatus. Signals were detected using a North2South chemiluminescent nucleic acid hybridization and detection kit. To study the migration of free transferrin in a 30% continuous iodixanol gradient, 1 μg of biotinylated human holotransferrin was diluted in 6 ml of homogenization buffer and mixed with 6 ml of 60% iodixanol. Centrifugation, fraction collection, and signal detection were performed as described above, except that each fraction was loaded directly onto the membrane. Dense endocytic vesicles were identified by acid β-galactosidase activity (16) using a FluoReporter LacZ/galactosidase quantitation kit (Molecular Probes) except for the modification to the reaction buffer (200 mM sodium citrate [pH 4.0], 0.1% Triton X-100:) (16).

**Thapsigargin inhibition of free nuclear movement of 10-kDa dextran.** Fixable Alexa Fluor 488-conjugated 10-kDa dextran was purchased from Molecular Probes. The thapsigargin inhibition experiment was performed as described previously (12), except that the dextran was introduced into cells through an Influx pinocytic cell-loading reagent (Molecular Probes) as described by the manufacturer. Cell samples were fixed and stained with Syto 64 red fluorescent dye and DAPI as described above and observed on a Applied Precision deconvolution microscope. The Syto 64 red color channel was eliminated prior to printing.

## RESULTS

**Fluorescent AAV shows a persistent perinuclear pattern after entering cells followed by slow nuclear entry.** Wild-type AAV was labeled with the green fluorescent dye Alexa Fluor 488. Electron microscopy, SDS-PAGE, Coomassie blue staining, and Western blotting of the AAV preparations indicated that there was no detectable contamination with Ad, cellular proteins, or degraded AAV capsid proteins (Fig. 1). The empty-to-full-particle ratio of the virus was approximately 3:7, as determined by electron microscopy (data not shown). Labeled virus gave the same Coomassie blue staining and Western pattern as unlabeled virus did (data not shown), and the calculated dye-to-virus ratio of labeled virus preparations was approximately 2, which is close to the values reported in previous studies (4, 34, 35) with fluorescently labeled AAV capsids. No significant effect on viral titer was seen following virus labeling (data not shown).

HeLa cells were infected by labeled AAV at 37°C for 10 min at an MOI of 10,000 particles per cell to allow internalization. Because of the limited time for which the cells were exposed to virus (10 min), only a fraction of the input virus successfully entered the cells. This fraction was estimated by slot blots of intracellular DNA after virus was removed and the cells had been washed and was found to be approximately 5%. Thus, the effective MOI was approximately 500 DNA-containing particles per cell. Unbound virus was removed by washing the cells, and the cells were incubated at 37°C for various times up to 48 h. Cell samples were counterstained with red Syto 64 dye, which allowed visualization of the whole cell (Fig. 2), and nuclei positions were detected by DAPI staining (data not shown).

In agreement with the findings of Bartlett et al. (4), we found that labeled virus quickly entered the cells and started to accumulate around cell nuclei within 2 h (Fig. 2A). Surprisingly, this perinuclear pattern of AAV persisted for at least 16 h. At 16 h postinfection, viral signal was detected in nuclei, and by 24 h postinfection, a significant amount of viral protein could be found inside nuclei. However, at 24 h (Fig. 2A) and at 48 h (data not shown), there was a significant decrease in the fluo-

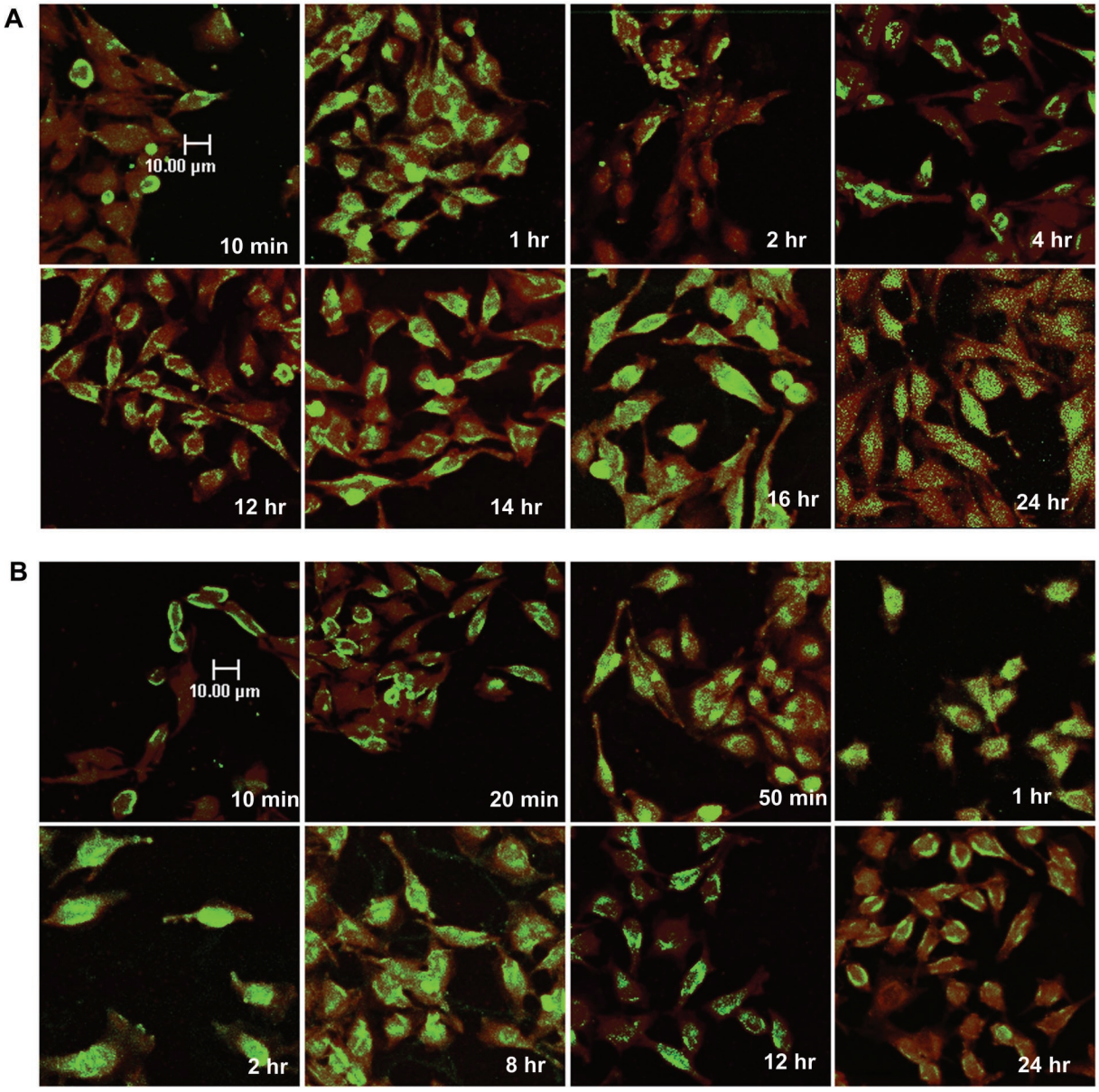


FIG. 2. Time course of AAV infection using fluorescently labeled virus. (A) HeLa cells were infected with Alexa Fluor 488-labeled AAV at a MOI of 10,000 particles per cell for 10 min at 37°C, washed to remove unadsorbed virus, and incubated at 37°C. Cell samples were taken at the indicated time points, stained with Syto 64 red fluorescent dye, and observed on a confocal microscope as described in Materials and Methods. (B) HeLa cells were incubated with Alexa Fluor 488 fluorescent dye only, and cell samples were taken at the indicated time points.

rescent signal, suggesting that the viral proteins had been degraded.

It has been our experience that dialysis alone is not sufficient to remove excess free dye from labeled virus preparations. Although we took care to remove free dye by heparin column chromatography (see Materials and Methods), it was still possible that contamination by trace amounts of free dye would confound interpretation of the study. We therefore performed a similar experiment with free Alexa Fluor 488 dye as a control (Fig. 2B). The control experiment clearly showed that within 2 h postinfection, almost all the free dye was localized in the nuclei, and after 8 h, free dye was excreted from the nuclei into the cytoplasm. By 24 h, the majority of the dye could be found only in the cytoplasm. The time course of the free dye experiment convinced us that free dye was not a significant contaminant in our preparations. Taken together, these experiments indicate that AAV particles, after entering the cells, quickly surround the cell nuclei and then enter slowly. It takes about 48 h for the majority of the capsid protein to enter the nuclei.

**Intact AAV particles do not appear to enter the nucleus.** Experiments with fluorescent-dye-labeled virus can provide information about the location of viral capsid proteins but do not indicate whether those viral capsids are still intact or already dissociated. To address this question, we applied an immuno-

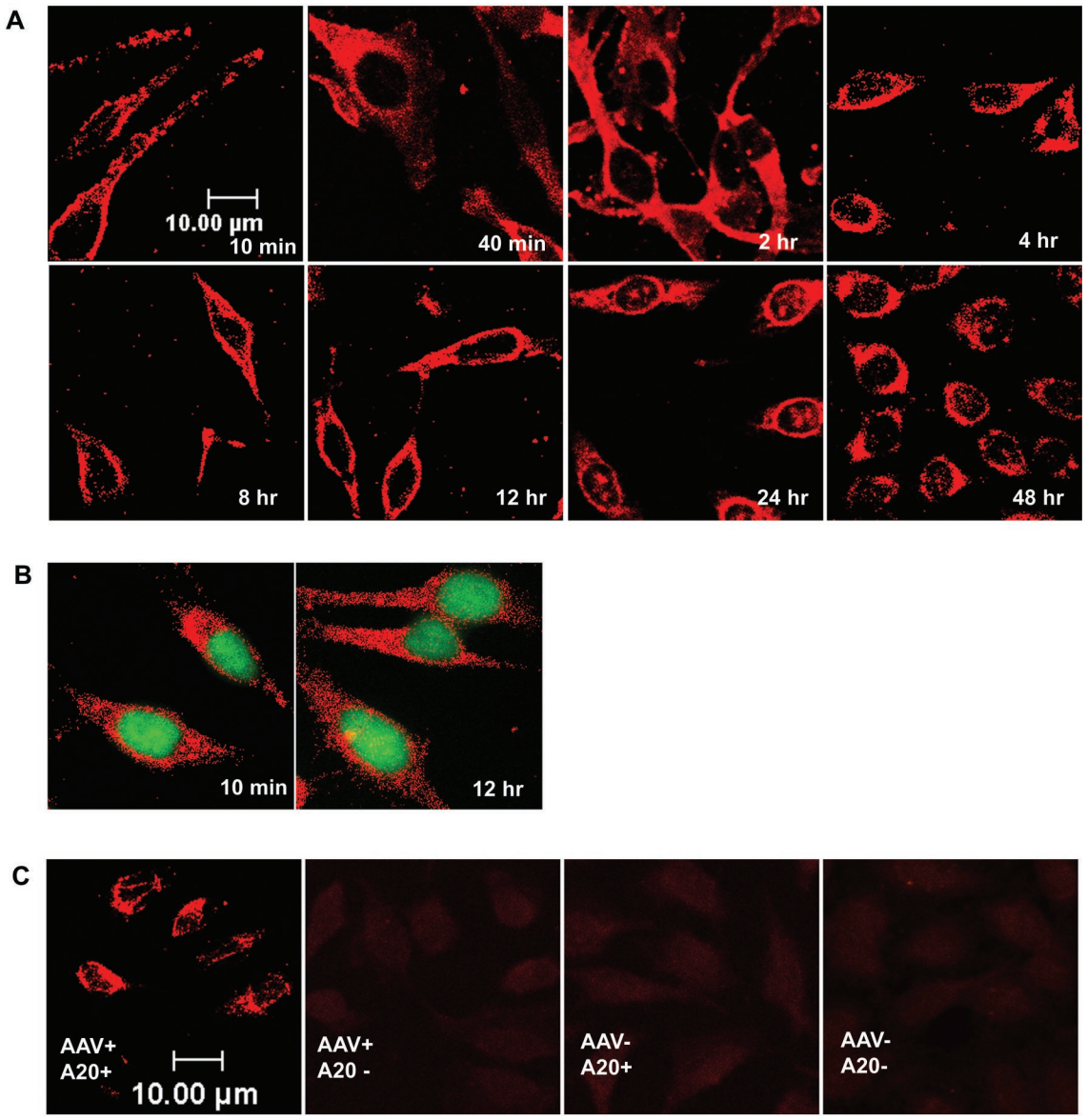


FIG. 3. Time course of AAV infection using A20 immunocytochemistry. (A) HeLa cells were infected with wild-type AAV at a MOI of 10,000 particles per cell for 10 min at 37°C, washed to remove unadsorbed virus, and incubated at 37°C. Samples were taken at the indicated time points, and intact viral particles were detected with A20 monoclonal antibody as described in Materials and Methods. (B) HeLa cells were infected with wild-type AAV as in panel A and incubated at 37°C for the indicated times. Samples were then stained with A20 antibody as in panel A and Syto X green, which stains nucleic acid in the nucleus. (C) Control A20 immunocytochemistry experiments. HeLa cells were infected with wild-type AAV or mock infected and then stained with A20 monoclonal antibody and Cy3-labeled goat anti-mouse Immunoglobulin G or just the secondary antibody.

cytochemistry method (Fig. 3) using A20 antibody, which specifically recognizes only intact AAV particles with a defined three-dimensional structure (46, 47). In the experiment in Fig. 3, only nondissociated AAV particles were detected by A20 antibody, giving rise to red signals when stained with a Cy3-coupled secondary antibody. Surprisingly, a majority of the intact viral particles persistently localized around cell nuclei throughout the 48-h experimental period, with little intact virus found inside the nuclei (Fig. 3A). To better visualize the nuclear boundary, the nucleic acid-specific dye Syto X green was used to stain the nuclei in some experiments (Fig. 3B). Taken together, the A20 and fluorescently tagged virus experiments suggested that intact virus did not enter the nucleus but that a significant portion of disrupted viral capsid proteins entered the nuclei after 16 h. Thus, the viral uncoating process must have happened shortly before or during the nuclear internalization of viral DNA for a majority of the input particles.

A few small clusters of intact AAV particles could be observed inside nuclei after 24 h postinfection (Fig. 3A). These could be the result of rare translocations of intact particles across the nuclear membrane, the result of particle reassembly from dissociated viral proteins (46), or the result of intact

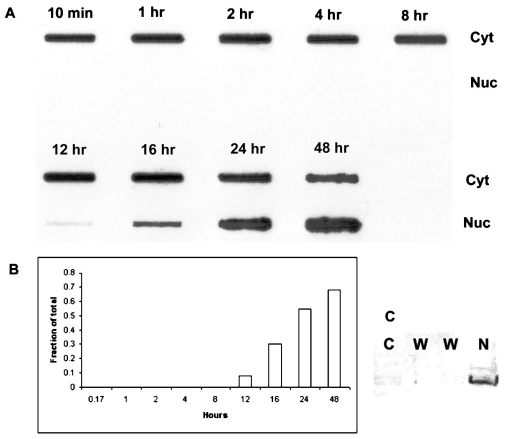


FIG. 4. Time course of AAV infection detected by DNA hybridization. (A) HeLa cells were infected with AAV as described in the legend to Fig. 3 and fractionated at the indicated time points into cytoplasmic (Cyt) and nuclear (Nuc) fractions. Viral DNA in each fraction was isolated and detected by slot blot hybridization. (B) The density of the DNA signals in the nucleus and cytoplasm was measured as described in Materials and Methods, and the fraction of the total DNA in the nucleus at each time point was calculated. (C) Western blotting of the cytoplasmic and nuclear fractions using anti-histone H3 antibody. C, cytoplasmic fraction; W, nuclear washes; N, nuclear fraction.

particles being trapped in nuclei following cell division. Because HeLa cells were infected at approximately 80% confluence in these experiments, a small fraction of the cells may have undergone division during the 48-h period. To ensure that our results were not an artifact of the antibody staining, we performed a control experiment (Fig. 3C), which showed that neither A20 nor the secondary antibody would give any signal when virus was not present.

**Viral DNA shows the same slow nuclear entry pattern as does fluorescent capsid protein.** Virus-infected cells were fractionated into nuclear and cytoplasmic fractions, and DNA hybridization was used to locate the viral DNA as a function of time after infection. In agreement with the data obtained with fluorescent dye-labeled virus (Fig. 2A), viral DNA was persistently localized in the cytoplasm of cells for an extended period after infection. Viral DNA was not detected in the nucleus until 12 h postinfection, and significant amounts of viral DNA were not present in the nucleus until 16 h, when the fraction of total viral DNA in the nucleus was 30% (Fig. 4A and B). The fraction of total DNA that appeared in the nucleus increased to approximately 70% by 48 h (Fig. 4B). This result confirmed our finding that after internalization, AAV particles rapidly accumulate outside nuclei but enter the nuclei slowly. No significant nuclear contamination was found in the cytoplasmic fractions as judged by Western blotting for histone H3 (Fig. 4C). Similarly, nuclear fractions were tested for cytoplasmic contamination by assaying for acid phosphatase, and it was found that less than 0.5% of the total acid phosphatase activity was occurring in the nuclear fraction (data not shown). These data suggest that AAV, after it accumulates perinuclearly, uncoats before or during the entry of viral DNA into nuclei.

**Ad coinfection significantly enhances the nuclear translocation of intact AAV particles.** Productive replication of AAV strongly depends on helper virus functions provided by either the Ad, or herpesvirus family (26). Although infection with the helper virus is not believed to affect rAAV entry or trafficking, in fact only early stages of viral entry have been examined (4). Therefore, we sought to determine whether coinfection with Ad might enhance intracellular trafficking of AAV. HeLa cells were infected with both AAV and Ad, and A20 immunocytochemistry and DNA slot blot analysis were performed as described above (Fig. 5 and 6). Surprisingly, in contrast to AAV infection without Ad, a substantial number of the intact AAV particles entered cell nuclei within 40 min postinfection (Fig. 5). DNA slot blot data supported the immunocytochemistry results and showed that viral DNA translocated from the cytoplasm to the nucleus starting at 40 min after the infection (Fig. 6A). By 1 h, approximately 25% of the viral DNA was present in the nucleus (Fig. 6B). After 8 h postinfection, in agreement with previous results (26), newly synthesized viral DNA was observed as judged by the fact that there was more nuclear DNA signal than input viral DNA (Fig. 6A, compare 10- and 40-min cytoplasmic signal to 12- to 48-h nuclear signal). The reduced amount of AAV DNA found in the 48-h nuclear sample was probably due to disruption of nuclei caused by Ad cytopathology. Our data suggested that in addition to overcoming the rate-limiting step of AAV DNA replication, i.e., second-strand DNA synthesis (9, 10), helper Ad can greatly enhance the nuclear translocation of intact AAV particles, another potentially rate-limiting step of AAV replication.

**Empty Ad capsids also facilitate AAV virus translocation to the nucleus.** Ad gene expression typically begins 1 h after infection (38). The rapid translocation of intact AAV capsids into the nucleus in the presence of Ad infection suggested that the Ad capsid itself may affect AAV trafficking. To determine if this was the case, we coinfected wild-type AAV and empty Ad capsids prepared from the Ad *ts*369 mutant. This mutant is defective in Ad DNA packaging due to a defect in the Ad L1 52/55K protein and produces only empty Ad capsids (18). As above, nuclear and cytoplasmic fractions were isolated at various times after infection and the time of appearance of AAV DNA in the nucleus was determined (Fig. 6C). AAV DNA appeared within the nucleus within 40 min after infection, essentially the same time course as seen with full wild-type Ad capsids. This suggested that empty Ad capsids were sufficient for facilitating AAV nuclear translocation. However, the rate of accumulation was significantly different from that seen in the presence of wild-type Ad, suggesting that perhaps expression of one or more Ad genes facilitated trafficking to the nucleus.

**AAV rapidly escapes from light endocytic organelles into the cytosol.** AAV enters cells through a receptor-mediated endocytosis pathway via clathrin-coated pits (7), and this endocytic processing is critical for efficient rAAV transgene expression (4, 6, 16). Previous studies had suggested either that AAV might be released from early endosomes into the cytoplasm (4, 35) or that it might traffic through a late-endosome compartment (6, 16). The pattern of trafficking was also suggested to be a function of cell type (6, 15, 16). To determine if Ad coinfection changed AAV trafficking in HeLa cells, we fractionated the nuclear free cytoplasmic fraction (PNS) by iodixanol den-

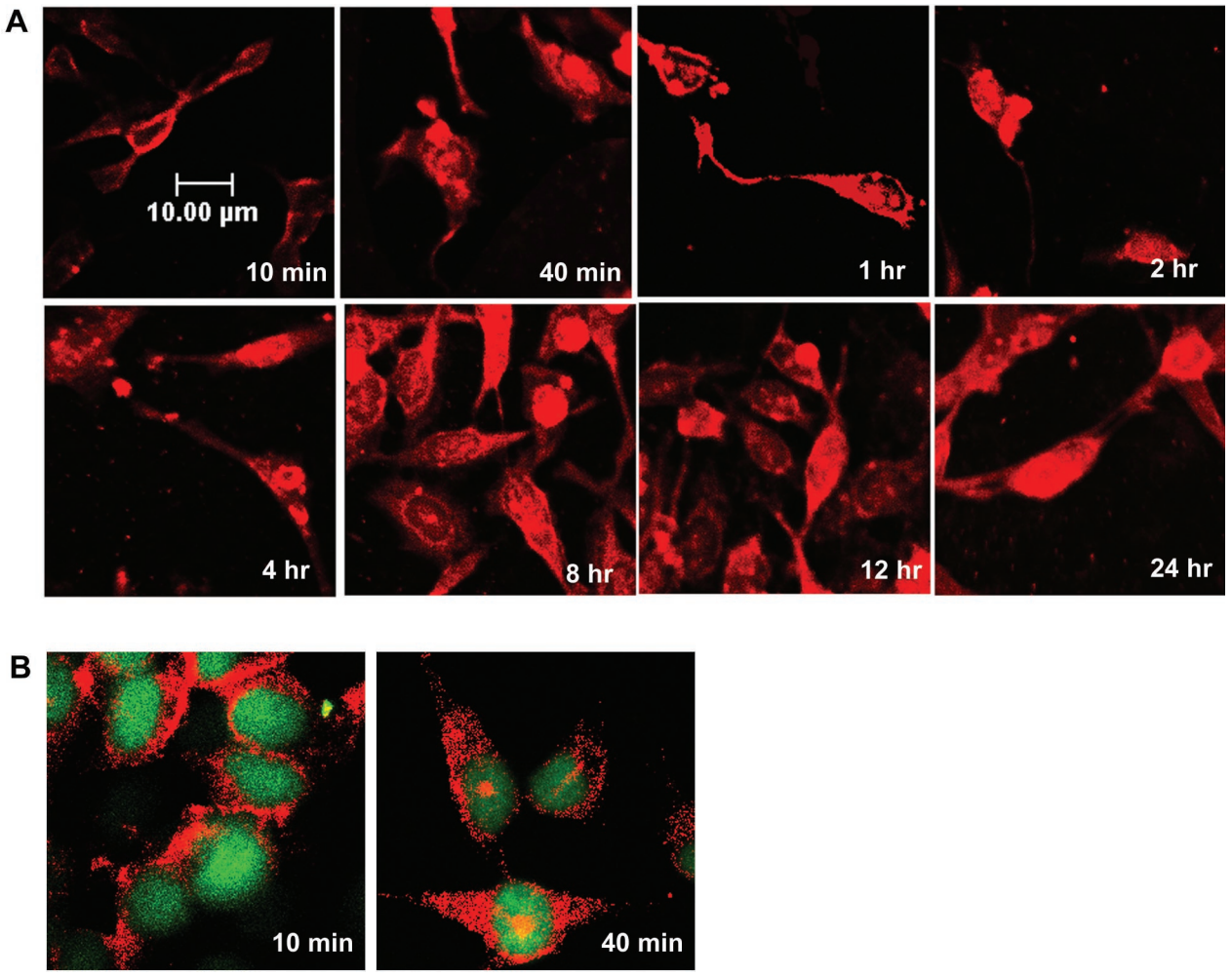


FIG. 5. Time course of AAV infection in the presence of Ad coinfection. HeLa cells were infected with wild-type AAV (MOI = 10,000 DNA-containing particles) and Ad5 (MOI = 10 PFU) for 10 min at 37°C and then washed to remove unabsorbed virus. The cells were then incubated with Ad5 (MOI = 10 PFU) for the duration of the experiment. Cell samples were taken at the indicated times postinfection and stained with A20 monoclonal antibody to visualize intact AAV particles as described in Materials and Methods. (B) HeLa cells were infected with wild-type AAV as in panel A and incubated at 37°C for the indicated time. Samples were then stained with A20 antibody as in panel A and Syto X green, which stains nucleic acid in the nucleus.

sity gradient centrifugation following infection with AAV alone or with AAV and Ad. Control experiments demonstrated that a 30% iodixanol gradient could clearly separate free virus (Fig. 7C, lane 1, fraction 2; density, 1.22 g/ml) from early endosomes that had been loaded with transferrin, an early-endosome marker (Fig. 7C, lane 3, fraction 12; density, 1.04 g/ml). Dense endocytic organelles were found at an intermediate density (less than 1.16 g/ml), as shown by the presence of acid β-galactosidase, a marker for dense endocytic vesicles (Fig. 7D). The positions of free viral DNA and free transferrin could also be separated (Fig. 7C, lanes 2 and 4).

After an initial 10-min incubation with HeLa cells, AAV was readily detected in the cytosol both in early endosomes and as free virus that was not associated with endocytic vesicles (Fig. 7A, lanes 10min to 8hr). Increasing the time of incubation at 37°C resulted in more virus that was free and less virus associated with early endosomes (Fig. 7A, fraction 2 versus fractions 11 and 12). As a consequence, the ratio of free virus to early-endosome-associated virus increased with time (Fig. 7B). No detectable virus or free DNA was associated with dense or late endosomes (Fig. 7A, fractions 3 to 10). When cells and virus were precooled to 4°C and maintained at 4°C throughout a 1-h incubation, little if any virus was associated with the cells after trypsinization (Fig. 7A, 4°C no entry lane). This presumably was because no endosomal uptake occurs at 4°C and virus bound to the cell surface was removed by trypsinization. When virus was added to cells at 37°C, immediately cooled to 4°C, and incubated for 1 h at 4°C, no free virus was seen and all of the virus was found trapped in the early-endosome compartment (Fig. 7A, lane 4°C entry lane). Taken together, these results confirmed earlier reports that virus could cross the cell membrane in 1 to 2 s and could enter the endosomal compartment in the range of milliseconds (35). Our data also confirm an earlier study with HeLa cells in which it was shown that virus escapes the early-endosome compartment within 10 min (4).

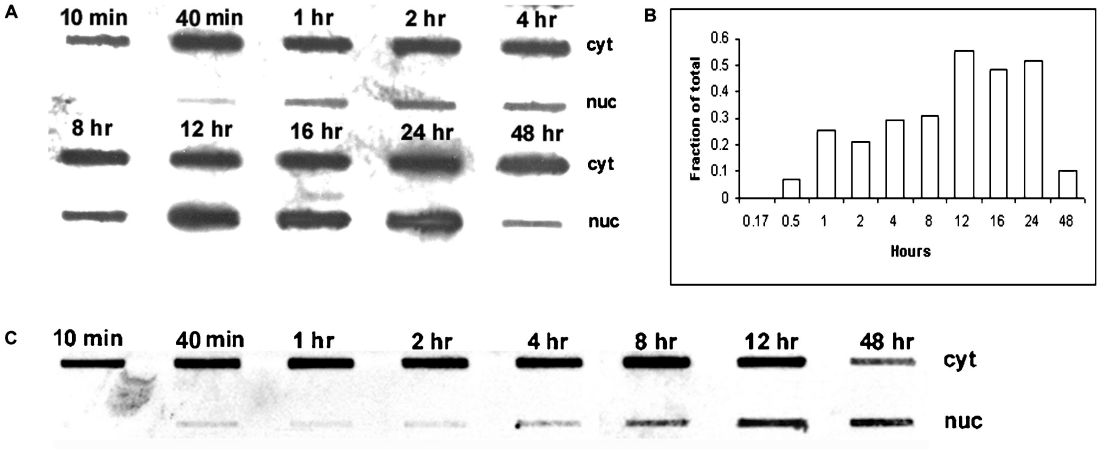


FIG. 6. Time course of viral DNA distribution in the presence of Ad coinfection. (A) HeLa cells were infected with AAV and Ad as described in the legend to Fig. 5. At the indicated times, cell samples were fractionated into nuclear (nuc) and cytoplasmic (cyt) fractions and viral DNA from each fraction was detected by slot blot hybridization. (B) The density of the DNA signals in the nucleus and cytoplasm was measured as described in Materials and Methods, and the fraction of the total DNA in the nucleus at each time point was calculated. (C) HeLa cells were infected with AAV and Ad as described in the Legend to Fig. 5, except that empty Ad5 *ts*369 particles (MOI = 1,000 particles) were used in place of wild-type Ad5. Cell samples were fractionated at the indicated times into nuclear and cytoplasmic fractions, and viral DNA was detected by slot blot hybridization.

Essentially the same trafficking pattern was found when cells were infected with AAV in the presence of Ad helper virus (Fig. 8). AAV was found both in the early-endosome form and as free virus, and the ratio of escaped virus to endosome-associated virus increased with time (Fig. 8). No virus DNA was found associated with the late-endosome fraction, suggesting that Ad does not alter the endocytic processing of AAV. However, because nuclear entry in the presence of Ad is dramatically enhanced, the amount of escaped virus found in PNS was significantly smaller than that seen without Ad coinfection (compare Fig. 8B and 7B). This result supported the conclusion that Ad facilitates AAV nuclear translocation after AAV escapes from the early endosome.

**An NPC inhibitor does not block Ad-facilitated AAV nuclear translocation.** Since Ad infection did not alter release of AAV from early endosomes, we speculated that it facilitated AAV translocation into the nucleus by changing the function of the NPC. To test this possibility, we blocked cellular NPCs with thapsigargin, an inhibitor of the endoplasmic reticulum/nuclear envelope-resident calcium pump that blocks movement through the nuclear pore when cells are maintained in calcium free medium (12, 20). In a control experiment, thapsigargin was shown to inhibit the NPC by blocking the nuclear movement of 10-kDa dextran fluorescently labeled with Alexa Fluor 488 (Fig. 9C), as described previously (12). However, when cells were infected with AAV in the presence of Ad, AAV DNA appeared in the nucleus as quickly as it did in the absence of the drug (Fig. 9A). The only difference was that AAV DNA replication, as judged by the increase in the level of nuclear AAV DNA over input values, appeared to be delayed by 12 h compared to the drug-free experiment (compare Fig. 9A and 6A). In addition, no Ad-induced cytopathic effect was observed for drug-treated cells at 48 h postinfection (data not shown). Presumably, the delay in AAV DNA replication and Ad cytopathology occurred because the Ad genome or nuclear proteins involved in these processes (for example, the AAV Rep protein) were blocked from nuclear entry through the NPC (13). When the $Ca^{2+}$-free medium was replaced by normal medium the normal AAV replication profile was restored (Fig. 9B). We interpreted these results to mean that AAV entry into the nucleus was not affected by thapsigargin, while AAV- and Ad-encoded enzymes and the Ad genome itself were delayed by 12 h.

## DISCUSSION

It is clear that AAV enters host cells through receptor-mediated endocytosis (4, 7, 30, 40, 41) and that viral DNA migrates to the nucleus, where DNA replication or integration occurs (26). It is not clear, however, when and where viral uncoating occurs, how the virus enters the nucleus, and whether Ad substantially changes the pattern of this trafficking. Indeed, there is some disagreement about these issues, and in some cases it appears that trafficking is a function of the cell type being studied (4, 6–8, 15–17, 34, 35). In this study, we have used fluorescent dye-labeled AAV to monitor viral capsid protein, DNA hybridization to trace viral DNA, and immunocytochemistry to localize intact AAV particles in HeLa cells in the presence and absence of Ad.

**Trafficking of AAV to the nucleus appears to be a slow process in the absence of Ad.** Previous studies of AAV entry had been confined to relatively short periods postinfection (less than 4 h). Our data indicate that in the absence of Ad, the major portion of viral protein and DNA stayed outside the cell nucleus for relatively long periods (up to 12 h postinfection). Subsequently, both labeled AAV capsid protein and DNA appeared in the nucleus in detectable amounts at 16 h postinfection. In contrast, intact, fully assembled AAV particles (as measured by A20 immunoreactivity) remained perinuclear throughout the 48-h experimental period (Fig. 3). These results suggest that nuclear entry of AAV in HeLa cells is a much

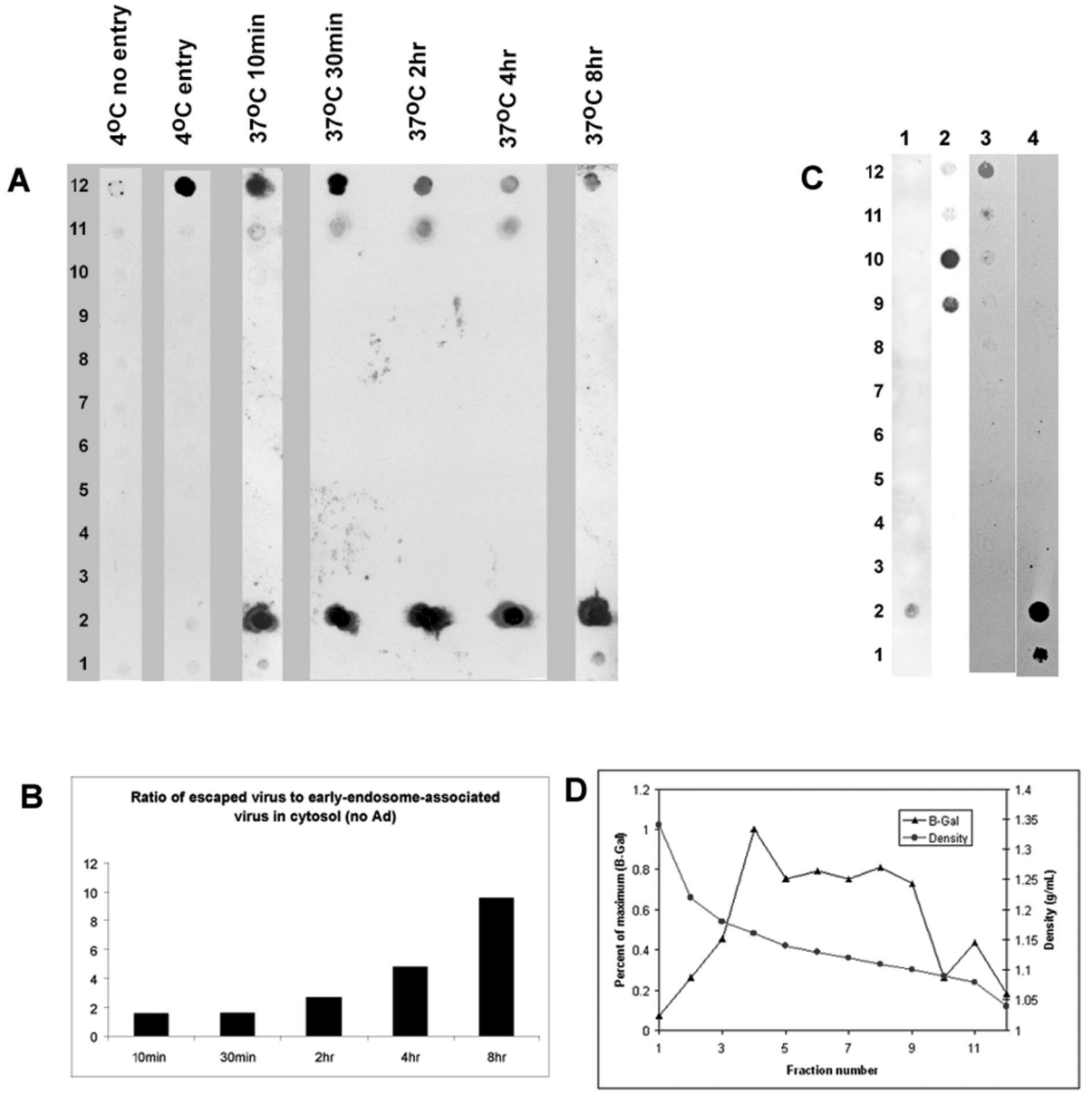


FIG. 7. Subcellular fractionation of AAV-infected cells. (A) HeLa cells were infected with AAV as described below, and the nucleus-free cytoplasmic fraction was fractionated on a continuous iodixanol gradient as described in Materials and Methods. Viral DNA was isolated from each fraction and detected by dot blot hybridization as described in Materials and Methods. Lanes: 4°C no entry, cells and virus were precooled to 4°C, and then cell samples were incubated at 4°C for 1 h; 4°C entry, AAV was added directly to warm cells, and then cells were incubated at 4°C for 1 h; 37°C 10min to 37°C 8hr; Cells were infected with AAV at 37°C and harvested at the indicated time. (B) The intensities of the free cytoplasmic virus (fraction 2) and early-endosome-associated virus signals (fractions 11 and 12) were scanned and plotted as the ratio of escaped to endosome-associated virus. (C) Continuous iodixanol gradients were loaded with AAV (lane 1), viral DNA isolated from purified AAV (lane 2), endosomally trapped biotinylated human transferrin (see Materials and Methods) (lane 3), or free biotinylated transferrin (lane 4). (D) The distribution profile of β-galactosidase (β-Gal) activity, a marker for dense endocytic vesicles, was determined on a continuous iodixanol density gradient. Density was determined by weight.

slower process than was previously appreciated and that viral uncoating occurs before or during viral nuclear translocation.

Interestingly, a similar long-term perinuclear accumulation pattern was also seen in AAV type 5 infections of HeLa cells (2) and in the case of canine parvovirus (CPV) (45). CPV capsids enter the nucleus between 6 and 8 h and continue to accumulate in the nucleus out to 12 h postinfection (45). However, in contrast to AAV, intact CPV capsids are capable of entering the nucleus.

**The pattern of AAV trafficking dramatically changed when Ad was present.** First, AAV capsids translocated into cell nuclei as intact particles in the presence of Ad. Second, the capsids appeared in the nucleus as early as 40 min postinfection, as shown by A20 immunocytochemistry and DNA hybrid-

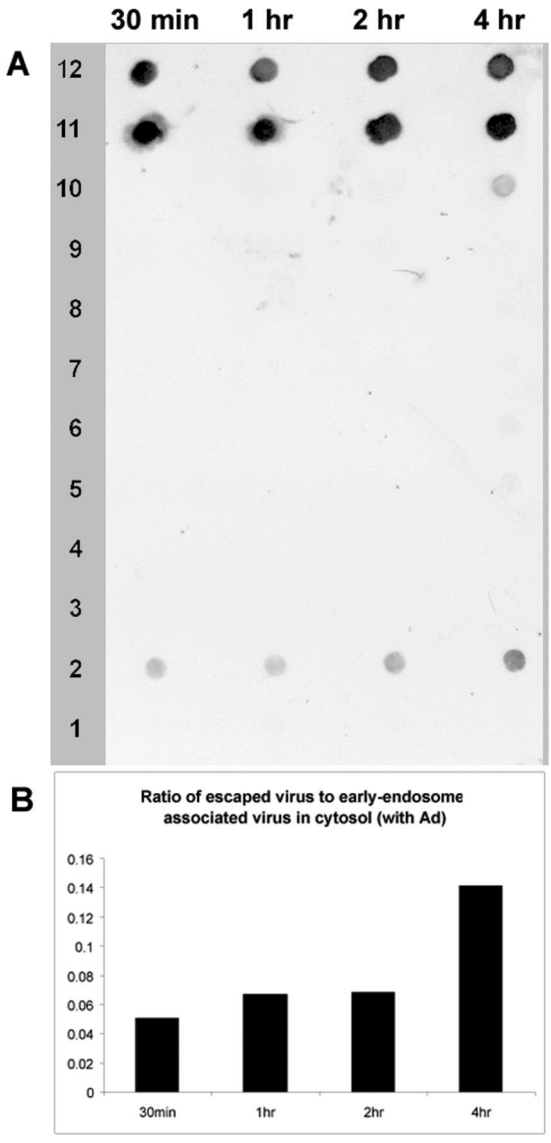


FIG. 8. Subcellular fractionation of cells coinfected with AAV and Ad. (A) Nucleus-free cytoplasmic extracts of AAV- plus Ad5-infected HeLa cells were taken at the indicated time points postinfection and subjected to continuous iodixanol gradient centrifugation as in Fig. 7. Viral DNA was detected by dot blot hybridization. (B) The intensities of the free cytoplasmic virus (fraction 2) and early-endosome-associated virus signals (fractions 11 and 12) were scanned and plotted as the ratio of escaped to endosome-associated virus.

ization (Fig. 5 and 6). This suggested that Ad infection changed the mechanism of AAV nuclear entry. Furthermore, the fact that intact AAV capsids entered the nucleus suggests that in the presence of Ad, AAV particles uncoat in the nucleus. The rapid accumulation of AAV in the nucleus suggested that Ad early-gene expression, which normally begins around 1 h postinfection, was probably not essential for AAV trafficking (38). A more likely explanation was that one or more proteins of the Ad capsid itself affected AAV trafficking. Indeed, this was confirmed by showing that empty Ad capsids were also capable of promoting early nuclear entry of AAV, although with different kinetics.

Ad enters cells with a $t_{1/2}$ of 2.5 min (22), escapes from early endosomes with a $t_{1/2}$ of 5 min by disrupting endosomes with its penton base (38), quickly undergoes a stepwise uncoating to release its structural proteins (within 10 to 15 min), and finally injects its DNA contents into the nuclei through the nuclear pore (14). More than 80% of Ad proteins are associated with nuclei within 1 h of infection (22).

Despite the rapid endosomal escape and nuclear accumulation of Ad, it is unlikely that Ad proteins directly assist AAV endosomal trafficking. First, AAV is able to leave early endosomes efficiently in the absence of Ad with approximately the same kinetics (Fig. 7 and 8) (4). Second, Bartlett et al. (4) have shown previously that Ad and AAV appear to enter cells through distinct endocytic pathways, so that the two types of capsids rarely localize to the same endosomes. An alternative explanation is that the Ad capsid induces a signal transduction pathway that changes AAV trafficking after escape from early endosomes. It has been shown recently that both active and transcription-defective Ad particles can induce extracellular signal-regulated kinase 1/2 and p38 kinase pathways at 10 and 20 min postinfection, respectively (43), as well as the Raf/mitogen-activated protein kinase signaling pathway (5). Induction of these pathways or some other signal transduction pathway could account for the altered AAV trafficking seen in the presence of Ad. Alternatively, Ad capsid proteins alter the integrity of cellular membranes (36, 37).

The existence of two alternative trafficking patterns, depending on whether Ad is present, is consistent with the life cycle of AAV. Ad lytic infections are essentially complete within 48 h. Thus, if AAV is to succeed in synthesizing a burst of particles, AAV DNA must be present in the nucleus by the time Ad early expression is finished. On the other hand, in the absence of Ad, AAV persists either as a provirus on chromosome 19 or as a nuclear episome. In either case, the virus is not under a time constraint for entering the nucleus in the absence of Ad. In fact, the slow entry process may help explain the common observation that AAV transduction requires 1 to 6 weeks to reach maximum expression depending on the type of tissue transduced (33).

**AAV appears to escape from early endosomes regardless of whether Ad is present.** Fractionation of cytoplasmic vesicles by density gradient centrifugation demonstrated that approximately half of the virus was released from the early-endosome fraction within 10 min after infection. Despite the rapid release of substantial amounts of virus from early endosomes, the remainder was released into cytoplasm over the next 8 h (Fig. 7). This may suggest that there are two different populations of endosome-associated virus. Similar results were observed in the presence of Ad (Fig. 8). We saw no evidence that AAV trafficked through a dense endocytic compartment. This is consistent with earlier reports that AAV is rapidly released from early endosomes (4) and that AAV exists either as an endosome-associated virus particle or as free virus in the cytoplasm (35). It is also consistent with reports that inhibition of proteosomal processing can alter AAV transduction and increase the amount of AAV DNA that enters the nucleus (6, 8). Our results are also in general agreement with the results of studies of CPV, which was found to colocalize with transferrin, an early endosome marker (28, 45). In contrast to the results presented here, AAV was found in both light (early) and dense

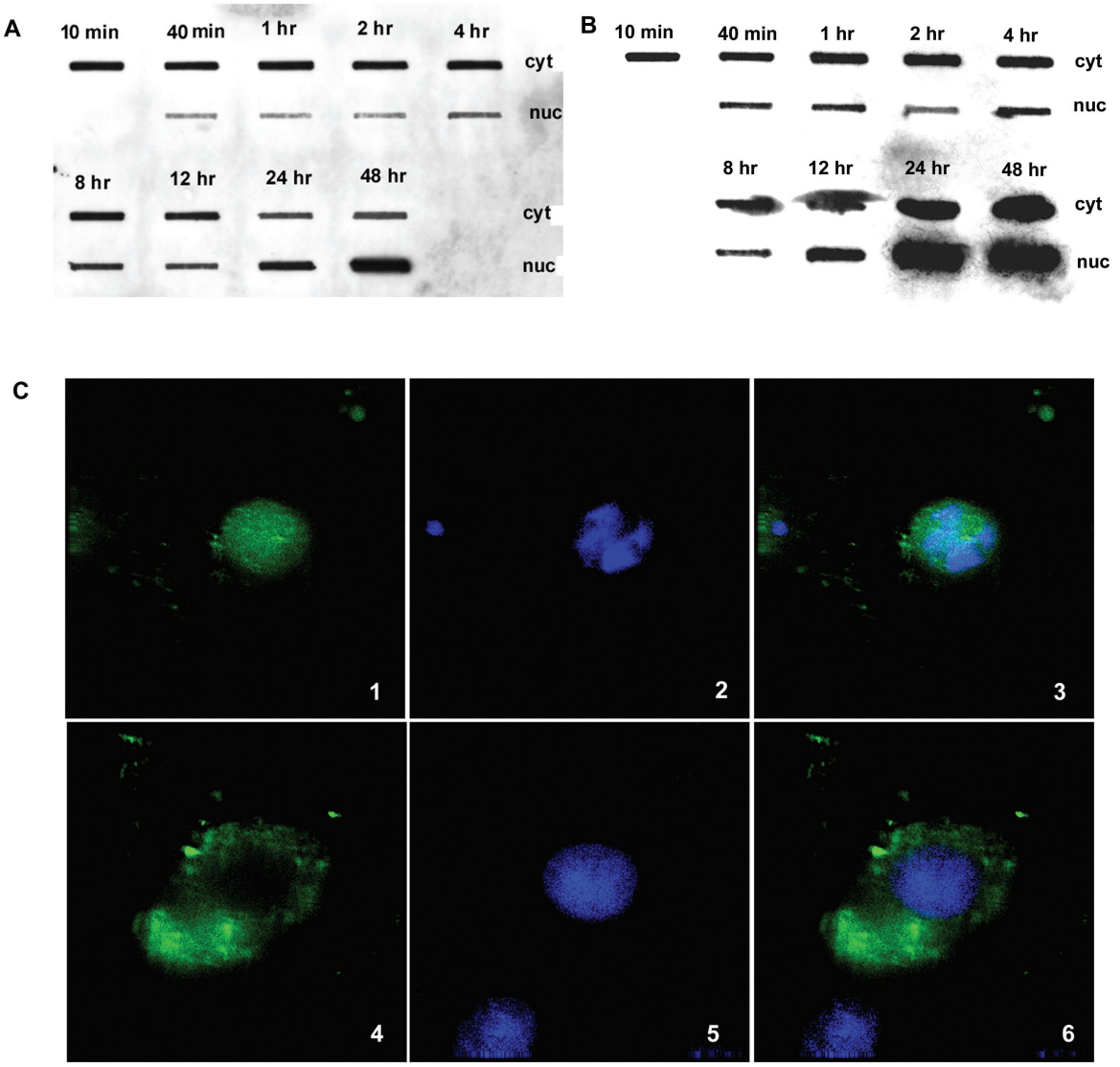


FIG. 9. Effect of the NPC inhibitor on AAV nuclear translocation in the presence of Ad. (A) Thapsigargin-treated cells were infected with AAV and Ad in $Ca^{2+}$-free S-MEM. Cell samples were taken at the indicated time points and fractionated into cytoplasmic (cyt) and nuclear (nuc) fractions. Viral DNA from each fraction was detected by slot blot hybridization. (B) Cells were treated the same way as in panel A but maintained in normal calcium-containing DMEM. (C) Thapsigargin inhibition of the nuclear movement of 10-kDa dextran. Alexa Fluor 488-conjugated 10-kDa dextran was introduced into HeLa cells as described in Materials and Methods. Nuclei were stained with DAPI, and samples were observed under deconvolution microscope. Panels: 1 and 4, labeled dextran; 2 and 5, DAPI stain; 3 and 6, merged. Panels 1 to 3 were not treated with thapsigargin; panels 4 to 6 were treated with thapsigargin.

(late) endocytic organelles of 293 cells but only in light endocytic vesicles of NIH 3T3 cells, although a substantial amount of free virus was found in both cell lines (16). We think that this probably reflects a difference in processing of AAV in 293 and NIH 3T3 cells compared to HeLa cells.

**AAV may not use the NPC for entry of intact capsids.** The NPC has a structural core consisting of a central transporter surrounded by a highly symmetrical spoke-ring complex; it is normally the only gateway for macromolecules to enter the nucleus (42). Eight 10-nm channels in the NPC allow the free movement of molecules as large as 50 kDa within 24 h, and the size limit of the NPC for signal-mediated active transport is around 26 nm (42), about the same size as AAV (26). To investigate the role of NPC in Ad-facilitated AAV nuclear translocation, we sought to determine the effect of thapsigargan, an NPC blocker that inhibits the endoplasmic reticulum/nuclear pore-resident calcium pump (12, 20), on the nuclear entry of AAV in the presence of Ad (Fig. 9). Our data show that the nuclear translocation of AAV in the presence of Ad was unaffected by the NPC blocker. However, AAV replication was delayed by 12 h, presumably because one or more Ad, AAV, or cellular proteins were blocked in nuclear entry. The block in AAV replication could be reversed by replacing the $Ca^{2+}$ in the medium. Taken together, our data suggested that AAV capsids entered the nuclei by some mechanism other than the NPC. Hansen et al. (17) also recently reported data

suggesting that AAV could enter nuclei by an NPC-independent pathway in isolated nuclei. We also note that a phospholipase activity has been identified in the capsid amino sequence that is unique to parvovirus VP1, a minor capsid protein. Mutation of the phospholipase motifs appeared to block infection of AAV and porcine parvovirus at the level of nuclear entry (11, 49).

In summary, our results suggest that AAV enters the cell rapidly and escapes from early endosomes within 10 min postinfection. In the absence of Ad, cytoplasmically distributed AAV accumulates outside the nucleus and viral uncoating occurs before or during the slow nuclear entry around 16 h postinfection. In the presence of Ad coinfection, cytosolic AAV quickly translocates into the nucleus as intact particles, and this process is not blocked by the NPC inhibitor thapsigargin. Further studies of the interaction of AAV with the nucleus are required to fully understand the infectious entry pathway of this virus.

## ACKNOWLEDGMENTS

We thank Mark Potter and Sergei Zolotukhin for advice on the production and characterization of AAV. We also thank Weijun Chen for making the Ad and Pei Wu for helpful discussions.

This work was supported by NIH grants PO1 HL51811 and P50 HL59412 to N.M., RO1 AG10485 to J.H., and RO1 AI41636 to P.H. and by the Edwin R. Koger Chair to N.M. N.M. is an inventor on patents related to recombinant AAV technology and owns equity in a gene therapy company that is commercializing AAV for gene therapy applications.

## REFERENCES

1. **Agbandje, M., T. C. Jenkins, R. McKenna, A. P. Reszka, and S. Neidle.** 1992. Anthracene-9,10-diones as potential anticancer agents. Synthesis, DNA-binding, and biological studies on a series of 2,6-disubstituted derivatives. J. Med. Chem. **35:**1418–1429.
2. **Bantel-Schaal, U., B. Hub, and J. Kartenbeck.** 2002. Endocytosis of adeno-associated virus type 5 leads to accumulation of virus particles in the Golgi compartment. J. Virol. **76:**2340–2349.
3. **Bartlett, J. S., and R. J. Samulski.** 1998. Fluorescent viral vectors: a new technique for the pharmacological analysis of gene therapy. Nat. Med. **4:**635–637.
4. **Bartlett, J. S., R. Wilcher, and R. J. Samulski.** 2000. Infectious entry pathway of adeno-associated virus and adeno-associated virus vectors. J. Virol. **74:**2777–2785.
5. **Bruder, J. T., and I. Kovesdi.** 1997. Adenovirus infection stimulates the Raf/MAPK signaling pathway and induces interleukin-8 expression. J. Virol. **71:**398–404.
6. **Douar, A. M., K. Poulard, D. Stockholm, and O. Danos.** 2001. Intracellular trafficking of adeno-associated virus vectors: routing to the late endosomal compartment and proteasome degradation. J. Virol. **75:**1824–1833.
7. **Duan, D., Q. Li, A. W. Kao, Y. Yue, J. E. Pessin, and J. F. Engelhardt.** 1999. Dynamin is required for recombinant adeno-associated virus type 2 infection. J. Virol. **73:**10371–10376.
8. **Duan, D., Y. Yue, Z. Yan, J. Yang, and J. F. Engelhardt.** 2000. Endosomal processing limits gene transfer to polarized airway epithelia by adeno-associated virus. J. Clin. Investig. **105:**1573–1587.
9. **Ferrari, F. K., T. Samulski, T. Shenk, and R. J. Samulski.** 1996. Second-strand synthesis is a rate-limiting step for efficient transduction by recombinant adeno-associated virus vectors. J. Virol. **70:**3227–3234.
10. **Fisher, K. J., G. P. Gao, M. D. Weitzman, R. DeMatteo, J. F. Burda, and J. M. Wilson.** 1996. Transduction with recombinant adeno-associated virus for gene therapy is limited by leading-strand synthesis. J. Virol. **70:**520–532.
11. **Girod, A., C. E. Wobus, Z. Zadori, M. Ried, K. Leike, P. Tijssen, J. A. Kleinschmidt, and M. Hallek.** 2002. The VP1 capsid protein of adeno-associated virus type 2 is carrying a phospholipase A2 domain required for virus infectivity. J. Gen. Virol. **83:**973–978.
12. **Greber, U. F., and L. Gerace.** 1995. Depletion of calcium from the lumen of endoplasmic reticulum reversibly inhibits passive diffusion and signal-mediated transport into the nucleus. J. Cell Biol. **128:**5–14.
13. **Greber, U. F., M. Suomalainen, R. P. Stidwill, K. Boucke, M. W. Ebersold, and A. Helenius.** 1997. The role of the nuclear pore complex in adenovirus DNA entry. EMBO J. **16:**5998–6007.
14. **Greber, U. F., M. Willetts, P. Webster, and A. Helenius.** 1993. Stepwise dismantling of adenovirus 2 during entry into cells. Cell **75:**477–486.
15. **Hansen, J., K. Qing, H. J. Kwon, C. Mah, and A. Srivastava.** 2000. Impaired intracellular trafficking of adeno-associated virus type 2 vectors limits efficient transduction of murine fibroblasts. J. Virol. **74:**992–996.
16. **Hansen, J., K. Qing, and A. Srivastava.** 2001. Adeno-associated virus type 2-mediated gene transfer: altered endocytic processing enhances transduction efficiency in murine fibroblasts. J. Virol. **75:**4080–4090.
17. **Hansen, J., K. Qing, and A. Srivastava.** 2001. Infection of purified nuclei by adeno-associated virus 2. Mol. Ther. **4:**289–296.
18. **Hasson, T. B., P. D. Soloway, D. A. Ornelles, W. Doerfler, and T. Shenk.** 1989. Adenovirus L1 52- and 55-kilodalton proteins are required for assembly of virions. J. Virol. **63:**3612–3621.
19. **Hirt, B.** 1967. Selective extraction of polyoma DNA from infected mouse cell cultures. J. Mol. Biol. **26:**365–369.
20. **Iborra, F. J., D. A. Jackson, and P. R. Cook.** 2001. Coupled transcription and translation within nuclei of mammalian cells. Science **293:**1139–1142.
21. **Kube, D. M., and A. Srivastava.** 1997. Quantitative DNA slot blot analysis: inhibition of DNA binding to membranes by magnesium ions. Nucleic Acids Res. **25:**3375–3376.
22. **Leopold, P. L., B. Ferris, I. Grinberg, S. Worgall, N. R. Hackett, and R. G. Crystal.** 1998. Fluorescent virions: dynamic tracking of the pathway of adenoviral gene transfer vectors in living cells. Hum. Gene Ther. **9:**367–378.
23. **Llamas-Saiz, A. L., M. Agbandje-McKenna, J. S. Parker, A. T. Wahid, C. R. Parrish, and M. G. Rossmann.** 1996. Structural analysis of a mutation in canine parvovirus which controls antigenicity and host range. Virology **225:**65–71.
24. **Maher, P. A.** 1996. Nuclear translocation of fibroblast growth factor (FGF) receptors in response to FGF-2. J. Cell Biol. **134:**529–536.
25. **McCarty, D. M., M. Christensen, and N. Muzyczka.** 1991. Sequences required for coordinate induction of adeno-associated virus p19 and p40 promoters by Rep protein. J. Virol. **65:**2936–2945.
26. **Muzyczka, N., and K. I. Berns.** 2001. Parvoviridae: the viruses and their replication, p. 2327–2360. *In* D. M. Knipe, P. M. Howley, and D. E. Griffin (ed.), Fields virology, 4th ed. Lippincott Williams & Wilkins, New York, N.Y.
27. **Nicklin, S. A., H. Buening, K. L. Dishart, M. de Alwis, A. Girod, U. Hacker, A. J. Thrasher, R. R. Ali, M. Hallek, and A. H. Baker.** 2001. Efficient and selective aav2-mediated gene transfer directed to human vascular endothelial cells. Mol. Ther. **4:**174–181.
28. **Parker, J. S., and C. R. Parrish.** 2000. Cellular uptake and infection by canine parvovirus involves rapid dynamin-regulated clathrin-mediated endocytosis, followed by slower intracellular trafficking. J. Virol. **74:**1919–1930.
29. **Potter, M., K. Chesnut, N. Muzyczka, T. R. Flotte, and S. Zolotukhin.** 2002. Streamlined large-scale production of recombinant adeno-associated virus (rAAV) vectors. Methods Enzymol **346:**413–430.
30. **Qing, K., C. Mah, J. Hansen, S. Zhou, V. Dwarki, and A. Srivastava.** 1999. Human fibroblast growth factor receptor 1 is a co-receptor for infection by adeno-associated virus 2. Nat. Med. **5:**71–77.
31. **Ruffing, M., H. Zentgraf, and J. A. Kleinschmidt.** 1992. Assembly of viruslike particles by recombinant structural proteins of adeno-associated virus type 2 in insect cells. J. Virol. **66:**6922–6930.
32. **Samulski, R. J., K. I. Berns, M. Tan, and N. Muzyczka.** 1982. Cloning of adeno-associated virus into pBR322: rescue of intact virus from the recombinant plasmid in human cells. Proc. Natl. Acad. Sci. USA **79:**2077–2081.
33. **Samulski, R. J., M. Sally, and N. Muzyczka.** 1998. Adeno-associated viral vectors. Cold Spring Harbor Laboratory Press, Cold Spring Harbor, N.Y.
34. **Sanlioglu, S., P. K. Benson, J. Yang, E. M. Atkinson, T. Reynolds, and J. F. Engelhardt.** 2000. Endocytosis and nuclear trafficking of adeno-associated virus type 2 are controlled by rac1 and phosphatidylinositol-3 kinase activation. J. Virol. **74:**9184–9196.
35. **Seisenberger, G., M. U. Ried, T. Endress, H. Buning, M. Hallek, and C. Brauchle.** 2001. Real-time single-molecule imaging of the infection pathway of an adeno-associated virus. Science **294:**1929–1932.
36. **Seth, P.** 1994. Adenovirus-dependent release of choline from plasma membrane vesicles at an acidic pH is mediated by the penton base protein. J. Virol. **68:**1204–1206.
37. **Seth, P., M. C. Willingham, and I. Pastan.** 1984. Adenovirus-dependent release of 51Cr from KB cells at an acidic pH. J. Biol. Chem. **259:**14350–14353.
38. **Shenk, T. E.** 2001. Adenoviridae: the viruses and their replication, p. 2265–2300. *In* D. M. Knipe, P. M. Howley, and D. E. Griffin (ed.), Fields virology, 4th ed, vol. 2. Lippincott Williams & Wilkins, New York, N.Y.
39. **Sperinde, G. V., and M. A. Nugent.** 1998. Heparan sulfate proteoglycans control intracellular processing of bFGF in vascular smooth muscle cells. Biochemistry **37:**13153–13164.
40. **Summerford, C., J. S. Bartlett, and R. J. Samulski.** 1999. AlphaVbeta5 integrin: a co-receptor for adeno-associated virus type 2 infection. Nat. Med. **5:**78–82.
41. **Summerford, C., and R. J. Samulski.** 1998. Membrane-associated heparan sulfate proteoglycan is a receptor for adeno-associated virus type 2 virions. J. Virol. **72:**1438–1445.

42. **Talcott, B., and M. S. Moore.** 1999. Getting across the nuclear pore complex. Trends Cell Biol. **9:**312–318.
43. **Tibbles, L. A., J. C. Spurrell, G. P. Bowen, Q. Liu, M. Lam, A. K. Zaiss, S. M. Robbins, M. D. Hollenberg, T. J. Wickham, and D. A. Muruve.** 2002. Activation of p38 and ERK signaling during adenovirus vector cell entry lead to expression of the C-X-C chemokine IP-10. J. Virol. **76:**1559–1568.
44. **Vihinen-Ranta, M., L. Kakkola, A. Kalela, P. Vilja, and M. Vuento.** 1997. Characterization of a nuclear localization signal of canine parvovirus capsid proteins. Eur. J. Biochem. **250:**389–394.
45. **Vihinen-Ranta, M., W. Yuan, and C. R. Parrish.** 2000. Cytoplasmic trafficking of the canine parvovirus capsid and its role in infection and nuclear transport. J. Virol. **74:**4853–4859.
46. **Wistuba, A., A. Kern, S. Weger, D. Grimm, and J. A. Kleinschmidt.** 1997. Subcellular compartmentalization of adeno-associated virus type 2 assembly. J. Virol. **71:**1341–1352.
47. **Wobus, C. E., B. Hugle-Dorr, A. Girod, G. Petersen, M. Hallek, and J. A. Kleinschmidt.** 2000. Monoclonal antibodies against the adeno-associated virus type 2 (AAV-2) capsid: epitope mapping and identification of capsid domains involved in AAV-2-cell interaction and neutralization of AAV-2 infection. J. Virol. **74:**9281–9293.
48. **Wu, P., W. Xiao, T. Conlon, J. Hughes, M. Aghandje-McKenna, T. Ferkol, T. Flotte, and N. Muzyczka.** 2000. Mutational analysis of the adeno-associated virus type 2 (AAV2) capsid gene and construction of AAV2 vectors with altered tropism. J. Virol. **74:**8635–8647.
49. **Zadori, S., J. Szelei, M.-C. Lacoste, Y. Li, S. Gariepy, P. Raymond, M. Allaire, I. Nabi, and P. Tijssen.** 2001. A viral phopholipase $A_2$ is required for parvovirus infectivity. Dev. Cell **1:**291–302.
50. **Zolotukhin, S., B. J. Byrne, E. Mason, I. Zolotukhin, M. Potter, K. Chesnut, C. Summerford, R. J. Samulski, and N. Muzyczka.** 1999. Recombinant adeno-associated virus purification using novel methods improves infectious titer and yield. Gene Ther. **6:**973–985.